Available online at www.sciencedirect.com
SCIENCE DIRECT®
Microporous and Mesoporous Materials 75 (2004) 255–260
MICROPOROUS AND MESOPOROUS MATERIALS
www.elsevier.com/locate/micromeso

Highly efficient nanocrystalline titania films made from organic/inorganic nanocomposite gels

Elias Stathatos [a], Panagiotis Lianos [a,*], Christos Tsakiroglou [b]

[a] *Engineering Science Department, University of Patras, GR-26500 Patras, Greece*
[b] *FORTH-ICE/HT, Stadiou Street, Platani, P.O. Box 1414, GR-26504 Patras, Greece*

Received 9 April 2004; received in revised form 8 July 2004; accepted 8 July 2004

Abstract

Thin transparent nanocrystalline titania films have been obtained from nanocomposite organic/inorganic gels by calcination at 550 °C. These gels have been deposited by the sol–gel process, where gelation is controlled by slow water release in the presence of ethanol and acetic acid while particle growth is controlled in the presence of the non-ionic surfactant Triton X-100. These titania films can attain high surface area (above 100 m^2/g) while maintaining high quality nanocrystallinity so that they become very efficient for various applications, including dye-sensitized solar cells and photodegradation.

Keywords: Titania; Films; Organic/inorganic nano composite; Gels

1. Introduction

Titania is one of the most interesting oxide semiconductors that finds increasing use in several application areas, such as solar cells, batteries, electrochromic devices, catalysts for organic pollutant photodegradation, etc. One very important aspect of TiO_2 preparation is its deposition as thin film on surfaces and electrodes. Highlights of the thus supported titania are its application to dye-sensitized photoelectrochemical solar cells (DSPEC) [1–4] and to coatings for environmental applications [5–10]. The present work actually targets these two interesting and popular applications. Its motive has been to synthesize titania films which possess two indispensable characteristics, that is, high active surface area and optical transparency, at the same time providing high photovoltaic efficiency when applied to solar cells, and high photodegradation capacity, when used in photocatalytic coatings for self-cleaning surfaces. The present work shows that optimal TiO_2 nanocrystalline films are easily obtained by calcinating nanocomposite organic/inorganic films synthesized by the sol–gel method. The procedure starts with a sol containing titanium isopropoxide ($Ti(OiPr)_4$), ethanol (EtOH), acetic acid (AcOH) and surfactant (Triton X-100).

A typical and best known sol–gel process is based on hydrolysis of an alkoxide, according to the reaction

$$Ti–OR + H_2O \rightarrow Ti–OH + ROH \quad (1)$$

where R is a short aliphatic group (isopropyl, in our case). The highly reactive Ti–OH thus created can polymerize (Ti–O–Ti) and lead to gelation only if it is kept in suspension. However, hydrolysis is exothermic and violent, particularly, in the case of transition metal alkoxides and usually it leads to undesirable routes, such as precipitation of particles of large size and uncontrollable shape and, generally to poor quality gels. It is then necessary to seek ways to make this process slow and controllable. There are several alternatives which have

* Corresponding author. Tel.: +30 2610 997587; fax: +30 2610 997803.
E-mail address: lianos@upatras.gr (P. Lianos).

1387-1811/$ - see front matter © 2004 Elsevier Inc. All rights reserved.
doi:10.1016/j.micromeso.2004.07.006

been proposed, including precipitant peptization [11], use of surfactant or polymer templates [12,13] reverse micelles [7,14], etc. Recent works choose to synthesize titania by slow water intake from the environment and from the water attached to the reagents in the precursor sol [15,16]. Very interesting results have also been obtained by introducing an organic acid in the sol [17,18], typically acetic acid, other organic acids being also applicable. In that case the sol–gel process includes several reaction routes, as can be seen by the following equations [2,17–19]:

$$\text{Ti–OR} + \text{AcOH} \rightarrow \text{Ti–OAc} + \text{ROH} \quad (2)$$

$$\text{ROH} + \text{AcOH} \rightarrow \text{ROAc} + \text{H}_2\text{O} \quad (3)$$

$$\text{Ti–OAc} + \text{ROH} \rightarrow \text{ROAc} + \text{Ti–OH} \quad (4)$$

$$\text{Ti–OR} + \text{Ti–OAc} \rightarrow \text{ROAc} + \text{Ti–O–Ti} \quad (5)$$

(In Reactions (2)–(5) as well as in the above Reaction (1), only one of four reacting alkoxy groups is taken into account, for reasons of simplicity.) Reactions (1)–(5) show that the end product of the sol–gel process, that is Ti–O–Ti, can be obtained by a colorful choice of chemical routes. Reaction (2), followed by (5) can lead to Ti–O–Ti, while water released through esterification Reaction (3) can yield oxide by the hydrolysis route. In the present work, where ethanol is introduced in the sol, even more water can be released by a direct EtOH–AcOH esterification reaction [18,19]. Furthermore, intermediate Ti–OAc ester or Ti–O–Ti oligomers may create entities which offer polymorphism to the sol–gel evolution. Thus the presence of a non-ionic surfactant, Triton X-100, which bears a chain of approximately 10 ether groups, plays a crucial role in organizing the structure of the material and in creating well defined and reproducible nanophases. As it has been previously shown [15], this family of surfactants participates in the formation and organization of clusters in solution, subsequently, organizing the structure of the ensuing gel. Slow water release, organic acid solvolysis and surfactant organization are then the key factors that dictate the structure and the quality of the nanocomposite gel and, subsequently, that of the ensuing nanocrystalline film.

2. Experimental

All reagents were from Aldrich except *cis*-bis(isothiocyanato)bis(2,2′-bipyridyl-4,4′-dicarboxylato)-ruthenium(II), abbreviated $RuL_2(NCS)_2$, which was provided by Solaronix SA (Switzerland). SnO_2:F transparent conductive electrodes (8 Ω/□) were purchased from Hartford Glass Co., USA.

2.1. Construction of titania films

Three grams of EtOH, various quantities of Triton X-100, 0.61 ml AcOH and 0.36 ml $Ti(OiPr)_4$ were mixed in this order under vigorous stirring and under ambient conditions. After 30 min stirring, a glass slide, previously cleaned in sulfochromic solution and sonicated in ethanol, was dipped in the sol, giving a uniform, transparent film. The film was then calcinated at 550 °C. The procedure was repeated 10 times. The thus obtained TiO_2 film was optically transparent, as can be seen by the absorption spectrum of Fig. 1. In this form, it was characterized by a few different techniques. When the films were prepared for DSPECs, the gel was deposited on commercial transparent conductive fluorine-doped SnO_2 (SnO_2:F) glasses.

2.2. Construction of dye-sensitized photoelectrochemical solar cells

Titania films were deposited on 8 Ω/□ SnO_2:F transparent conductive glasses. When the TiO_2 film was taken out of the furnace and while it was still hot, it was dipped into an 1 mM ethanolic solution of $RuL_2(NCS)_2$, and was left there overnight. Then the dye-coated electrode was copiously washed with ethanol and dried in a stream of N_2. The counter electrode was a slightly platinized SnO_2:F transparent conductive glass slide. Platinum was thermally evaporated in a vacuum chamber. It formed a very thin layer which very slightly affected the electrode transparency. The two electrodes were stucked together face to face by using silicon glue at the periphery of the cell. They were squeezed together

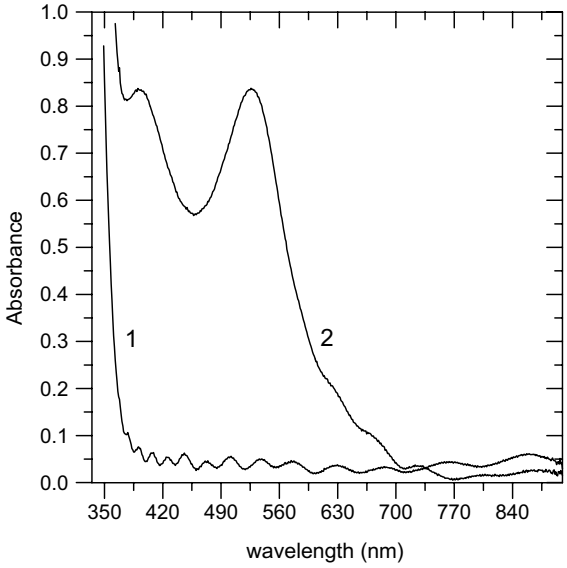

Fig. 1. Absorption spectra of the titania film with the smallest nanocrystallites (15 %wt Triton X-100): (1) pure; and (2) with adsorbed $RuL_2(NCS)_2$.

so they were virtually in conduct, the silicon glue providing a space of less than 10 μm. In between, an electrolyte was introduced by exploiting capillary forces. The electrolyte was 0.3 M LiI + 0.03 M I_2 dissolved in acetonitrile containing a few drops of pyridine [20].

2.3. Apparatus and measuring methods

UV–vis absorption measurements were made with a Cary 1E spectrophotometer. SEM images were obtained with a Jeol JSM 6300 microscope equipped with an EDS detector for elemental analysis (Oxford). X-ray diffraction measurements (XRD) were made with a Philips PW 1840 diffractometer. Atomic force microscopy (AFM) images were obtained with a Nanoscope III, Digital Instruments, in the tapping mode. Nitrogen, Brunauer–Emmett–Teller, (BET) measurements on titania films were made by using a high resolution Quantachrome Autosorb 1-C apparatus. *IV* curves have been recorded by connecting the cell to an external variable resistor and by measuring the current flowing through the resistor and the corresponding voltage across the resistor. The cell dimension for these measurements was 1 cm^2. Illumination was done by an Oriel 450 W Xenon lamp. Illumination intensity was controlled by multiple wire grids and it was 100 mW/cm^2. The same illumination source was employed for photodegradation experiments.

3. Results and discussion

3.1. Characterization of titania films

The thickness of the titania film of Fig. 1 was measured by using a scanning electron microscope image of a cross-sectional view of the film and was found to be 1.9 μm. Using this value and the interference fringes of Fig. 1, the refraction index was calculated and was found to be 1.92. The as-prepared films were characterized by X-ray diffraction. A typical diffractogramm is shown in Fig. 2, which reveals that the film in question consists of anatase containing 35% rutile. Interestingly, it was found that the presence of even a small quantity of Triton X-100 always results in a mixture of anatase and rutile. When no surfactant is added to the original sol the ensuing X-ray diffractogramme shows that films consist of pure anatase. By using the Scherrer formula [21] $\beta = \frac{k\lambda}{s\cos\theta}$, where β (radians) is the full-width at half-maximum in the 2θ scan, k is a constant (0.94), λ is the X-ray wavelength (1.54 Å for Cu Kα), s is the particle diameter and θ is the angle of the diffraction peak (degrees), it is possible to calculate the size of the nanocrystals which reflects on the width of the main X-ray diffraction peak. It has been found that the quantity of surfactant in the sol affects the size of the ensuing nanocrystallites as can be seen from the data of Table 1. The smallest size nanocrystallites were obtained when the quantity of Triton X-100 in the original sol was 15 %wt. Their value systematically decreased as the quantity of surfactant in the sol increased achieving a minimum at the above surfactant content. For further surfactant addition nanocrystallite size rapidly increased marking a sharp minimum at 15 %wt Triton X-100 content. Interestingly, the average size of the nanoparticles

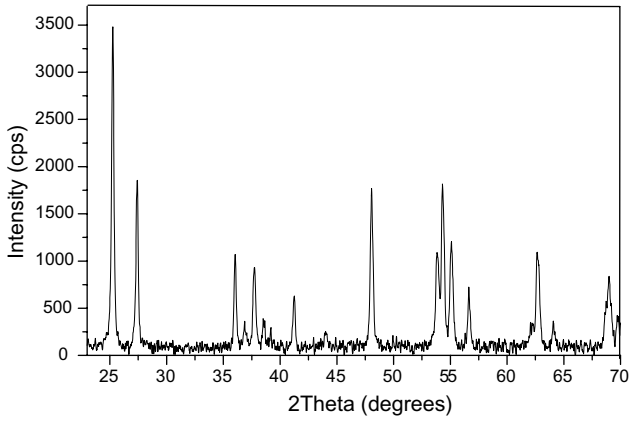

Fig. 2. XRD diffractogramm of the film with the smallest nanocrystallites (15 %wt Triton X-100).

Table 1
Data obtained by different characterization methods of titania films made at various surfactant percentages

Triton X-100 %wt	XRD	AFM measurements			BET data						Dye adsorption
	Particle diameter (nm)	Mean diameter (nm)	RMS roughness (nm)	Fractal dimension D_s	S (m^2/g)	V_p (cm^3/g)	R_{por} (nm)	R_{thr} (nm)	R_{app} (nm)	Fractal dimension D_s	Optical absorbance
0	–	–	–	–	38.9	0.115	4.36	3.02	5.9	1.85	0.07
2.5	14	14–16	0.736	2.201	–	–	–	–		–	0.44
5.0	12	12–14	1.070	2.333	76.0	0.198	3.98	2.44	5.2	2.11	0.45
10.5	12	12–14	1.036	2.369	–	–	–	–		–	0.69
15.0	11	10–13	1.190	2.368	107.1	0.173	3.62	2.30	3.2	2.10	0.82
17.5	15	17–19	1.031	2.391	63.2	0.117	3.24	2.53	3.7	2.19	0.56

S (m^2/g): BET surface area, V_p (cm^3/g): specific pore volume, R_{por} (nm) and R_{thr} (nm): pore and throat radii, respectively. $R_{app} = 2V_p/S_p$ (nm): apparent pore radius.

measured by AFM, (shown in Table 1), was very close to that measured by XRD. This fact simply means that the titania nanoparticles obtained by the above method are "ideal" nanocrystallites so that calculated and real sizes are very close. The AFM image of the film made of the minimum-size nanocrystallites is shown in Fig. 3. Obviously, the film consists of small nanocrystallites of narrow size distribution. As seen in Table 1, variation of the nanoparticle size with surfactant content, as extracted from AFM images, demonstrated the same trend as that detected by XRD. AFM data offered additional information concerning film roughness and fractal dimension. Roughness and fractal dimension of the film increased when the size of the nanoparticles decreased. Roughness achieved a maximum when the surfactant content was 15 %wt while fractal dimension further increased for further surfactant addition.

Table 1 also presents nitrogen BET data obtained by analyzing titania films. BET measurements are usually performed on powder samples of much larger sample quantity than that in thin films. However, by using a high resolution apparatus, it was possible to characterize thin titania films. The BET data of Table 1 have been obtained by analyzing the N_2 adsorption-desorption isotherms: the specific surface area (S) was determined by fitting low pressure data to the BET equation; the mean pore, R_{por} (void space left between particles) and throat, R_{thr} ("windows" interconnecting pores) radii were calculated for the relevant distributions which were obtained by taking into account the Kelvin and Frenkel–Halsey–Hill (FHH) equations, and by differentiating the N_2 adsorption and desorption isotherms, respectively [22]; an apparent pore radius, R_{app}, was estimated by using the approximate relationship $R_{app} = 2V_p/S_p$; and the BET surface fractal dimension was determined by fitting N_2 adsorption data to the fractal version of the FHH type equation [23]. The calculated total surface S dramatically increased when the surfactant content in the sol increased achieving a maximum at 15 %wt Triton X-100, i.e., at the same concentration where the size of the particles was the smallest and their roughness the highest. For further surfactant addition, S abruptly decreased, marking a sharp maximum at the above determined crucial surfactant content. The fractal dimension calculated by BET data gave different values than AFM data but both showed the same trend, i.e., they increased with surfactant concentration. Pore volume V_p, mean pore radius R_{por} and mean throat radius R_{thr} also varied with surfactant concentration, whereas the R_{app} values demonstrated the same trend as the particle size. The data of Table 1 lead to a clear conclusion. The presence of surfactant Triton X-100 affects the structure of the films in a decisive manner. Under the above conditions, it was made possible to determine a surfactant concentration (15 %wt) for which the nanocrystalline film contains the smallest nanocrystallites and possesses very large surface area, i.e., 107 m^2/g. This value is the highest ever recorded for calcinated nanocrystalline titania films [11,21]. The high surface area achieved with the above films was rewarded by the results, when the films were employed with targeted applications, as exposed in the following paragraphs.

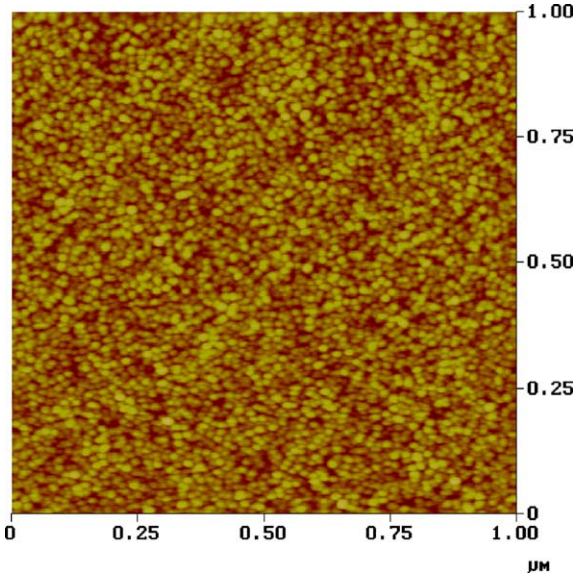

Fig. 3. AFM image of the film with the smallest size nanocrystallites (15 %wt Triton X-100).

3.2. Applications to dye-sensitized photoelectrochemical solar cells (DSPEC)

As can be seen in the last column of (Table 1), the above titania films can be loaded with a high amount of a dye sensitizer. *Cis*-bis(isothiocyanato)bis(2,2′-bipyridyl-4,4′-dicarboxylato)-ruthenium(II), $RuL_2(NCS)_2$, a typical dye employed with DSPECs, was optimally adsorbed to give absorbance equal to 0.82, i.e., about 85% absorbance at the maximum absorption wavelength (cf. Fig. 1). This is a pure photon intake, since the titania substrate is transparent in the visible, so all visible light is absorbed by the dye itself. Maximum adsorbance of $RuL_2(NCS)_2$ was obtained for 15 %wt Triton X-100, i.e., for the films where nanocrystallites were the smallest and the active surface area the largest. N_2 and dye adsorption data then followed the same trends. DSPECs made with titania deposited on fluorine doped SnO_2 transparent conductive electrodes, employing $RuL_2(NCS)_2$ as photosensitizer, a liquid I_3^-/I^- redox electrolyte and a platinized counter electrode gave an overall efficiency of 9.1%, as can be extracted from the I–V curve of Fig. 4. This efficiency is very high and it is comparable with that obtained with cells where relatively thick, virtually opaque, titania films were employed [20,24]. This efficiency can be further

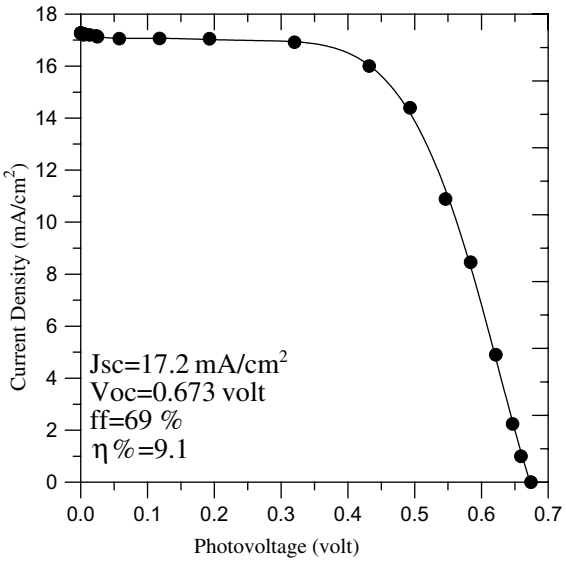

Fig. 4. *I–V* curve for a cell constructed with the optimal titania film. Size of the cell 1 cm^2. Illumination intensity 100 mW/cm^2.

improved by optimizing the rest of the components of the cell. The efficiency of the present films, which are transparent and relatively thin, is due to the optimal conditions of their deposition. The films possess high active surface area and well formed nanocrystallites, of uniform size, low size polydispercity, apparently with a minimum number of defects. Mixture of anatase and rutile brings more stability to the films since rutile is thermodynamically a more stable crystalline phase. Their transparency leaves space for their use in photovoltaic windows, which can be integrated in building architecture.

3.3. Photodegradation of a dye adsorbed on titania films

The above transparent and highly adsorbent films are equally successful when used as coatings on photocatalytic surfaces employed with photodegradation installations [7,25]. Films immersed in a dye solution and exposed to light are very efficient in decoloration under solar light illumination. Titania films made by the above procedure were immersed in an aqueous solution of Basic Blue 41 (for chemical structure see inset in Fig. 5a). The films were immediately deeply colored. The adsorbance of Basic Blue 41 on optimal titania films is so high that the films become virtually opaque (absorbance 3.0, transmittance 0.1%, cf. Fig. 5a). When the films were exposed to light produced by a xenon lamp, modulated to simulate the radiation of about 1 sun (100 mW/cm^2), the dye was rapidly photodegraded in a very short time (see Fig. 5b). Fig. 5b shows the evolution of visible light absorbance of the adsorbed dye. Eighty percent of the dye was decolored

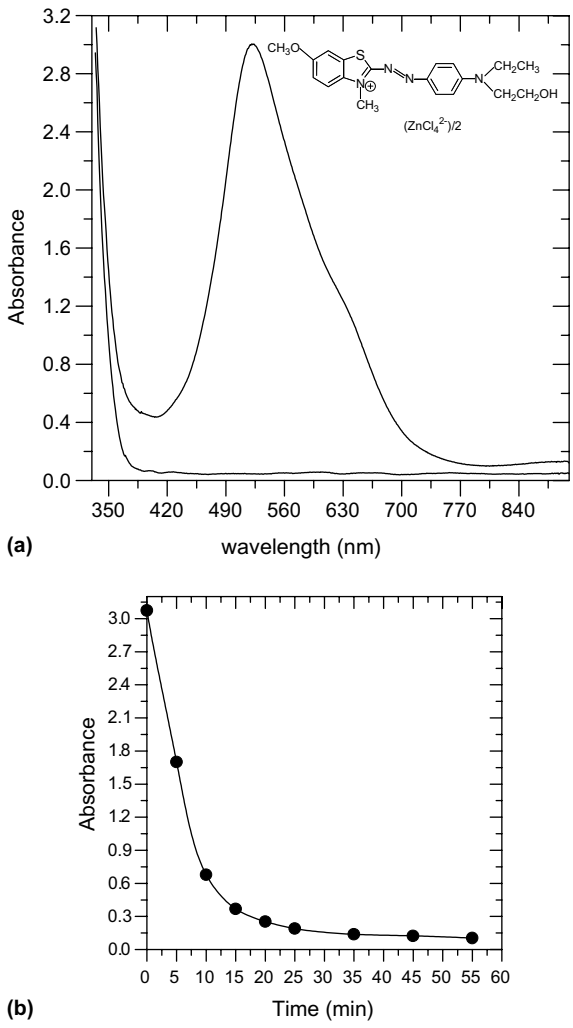

Fig. 5. Titania film with and without adsorbed Basic Blue (a) and photodegradation by simulated solar radiation (b).

in only 10 min, while any trace of the dye disappeared within an hour.

4. Conclusions

Nanocomposite organic/inorganic films deposited by the sol–gel method, using a sol containing titanium isopropoxide, ethanol, acetic acid and surfactant Triton X-100, can yield highly efficient nanocrystalline titania films by calcination at 550 °C. The efficiency of the films was demonstrated by two characteristic applications, i.e., in dye-sensitized solar cells, and in rapid photodegradation of adsorbed dye. The films consist of anatase nanocrystallites of uniform size containing a rather high percentage of rutile (35% in the optimal case). Optimal titania films possess very high active surface area which raised up to about 107 m^2/g, a value which is very high for films calcinated at such high temperatures.

Acknowledgments

We acknowledge financial support from Greece-Slovenia R&T Cooperation Program. We are deeply indebted to Dr. P. Falaras of the NRC Demokritos, Athens, Greece, for the AFM measurements, Prof. P. Koutsoukos of the Chemical Engineering Department, University of Patras, Greece for the XRD and SEM measurements and to Prof. B. Orel of the National Institute of Chemistry, Ljubljana, Slovenia for very fruitful discussions.

References

[1] B. O'Regan, M. Graetzel, Nature 353 (1991) 737.
[2] E. Stathatos, P. Lianos, U. Lavrencic-Stangar, B. Orel, Adv. Mater. 14 (2002) 354.
[3] K. Tennakone, P.V.V. Jayaweera, P.K.M. Bandaranayake, J. Photochem. Photobiol. A: Chem. 158 (2003) 125.
[4] S. Murai, S. Mikoshiba, H. Sumino, S. Hayase, J. Photochem. Photobiol. A: Chem. 148 (2002) 33.
[5] C. Longo, J. Freitas, M.-A. De Paoli, J. Photochem. Photobiol. A: Chem. 159 (2003) 33.
[6] E. Stathatos, T. Petrova, P. Lianos, Langmuir 17 (2001) 5025.
[7] P. Bouras, E. Stathatos, P. Lianos, C. Tsakiroglou, App. Catal. B: Environ. 51 (2004) 275.
[8] G. Balasubramanian, D.D. Dionysiou, M.T. Suidan, V. Subramanian, I. Baudin, J.-M. Laine, J. Mater. Sci. 38 (2003) 823.
[9] A. Mills, G. Hill, S. Bhopal, I.P. Parkin, S.A. O'Neill, J. Photochem. Photobiol. A: Chem. 160 (2003) 185.
[10] K. Nagaveni, M.S. Hedge, N. Ravishankar, G.N. Subbana, G. Madras, Langmuir 20 (2004) 2900.
[11] S.D. Burnside, V. Shklover, C. Barbe, P. Comte, F. Arendse, K. Brooks, M. Gratzel, Chem. Mater. 10 (1998) 2419.
[12] D.M. Antonelli, Micropor. Mesopor. Mater. 30 (1999) 315.
[13] L. Kavan, J. Rathousky, M. Graetzel, V. Shklover, A. Zukal, Micropor. Mesopor. Mater. 44 (2001) 653.
[14] E. Stathatos, P. Lianos, F. Del Monte, D. Levy, D. Tsiourvas, Langmuir 13 (1997) 4295.
[15] O. Dag, I. Soten, O. Helik, S. Polarz, N. Coombs, G.A. Ozin, Adv. Funct. Mater. 13 (2003) 30.
[16] E. Stathatos, P. Lianos, P. Falaras, Progr. Colloid Polym. Sci. 118 (2001) 96.
[17] D.P. Birnie III, N.J. Bendzko, Mater. Chem. Phys. 59 (1999) 26.
[18] C. Wang, Z.X. Deng, Y. Li, Inorg. Chem. 40 (2001) 5210.
[19] M. Ivanda, S. Music, S. Popovic, M. Gotic, J. Mol. Struct. 480–481 (1999) 645.
[20] M.K. Nazeeruddin, A. Kay, I. Rodicio, R. Hamphry-Baker, E. Mueller, P. Liska, N. Vlachopoulos, M. Graetzel, J. Am. Chem. Soc. 115 (1993) 6382.
[21] S. Nakade, M. Matsuda, S. Kambe, Y. Saito, T. Kitamura, T. Sakata, Y. Wada, H. Mori, S. Yanagida, J. Phys. Chem. B. 106 (2002) 10004.
[22] S.I. Gregg, K.S.W. Sing, Adsorption Surface Area and Porosity, Academic Press, London, 1982.
[23] B. Sahouli, S. Blacher, F. Brouers, Langmuir 12 (1996) 2872.
[24] M. Graetzel, Nature 414 (2001) 338.
[25] V. Subramanian, P.V. Kamat, E.E. Wolf, Ind. Eng. Chem. Res. 42 (2003) 2131.